SCIENTIFIC REPORTS

OPEN

SUBJECT AREAS:
QUANTUM INFORMATION
QUBITS

Received
11 September 2014

Accepted
9 December 2014

Published
13 January 2015

Correspondence and requests for materials should be addressed to W.Y. (ywl@wipm.ac.cn); X.Z. (xbzhu@aphy.iphy.ac.cn) or M.F. (mangfeng@wipm.ac.cn)

One-step generation of multipartite entanglement among nitrogen-vacancy center ensembles

Wan-lu Song[1,2], Zhang-qi Yin[3], Wan-li Yang[1], Xiao-bo Zhu[4,5], Fei Zhou[1] & Mang Feng[1]

[1]State Key Laboratory of Magnetic Resonance and Atomic and Molecular Physics, Wuhan Institute of Physics and Mathematics, Chinese Academy of Sciences, Wuhan 430071, China, [2]University of the Chinese Academy of Sciences, Beijing 100049, China, [3]Center for Quantum Information, Institute for Interdisciplinary Information Sciences, Tsinghua University, Beijing 100084, China, [4]The Institute of Physics, Chinese Academy of Sciences, Beijing 100190, China, [5]Collaborative Innovation Center of Quantum Matter, Beijing 100190, China.

We describe a one-step, deterministic and scalable scheme for creating macroscopic arbitrary entangled coherent states (ECSs) of separate nitrogen-vacancy center ensembles (NVEs) that couple to a superconducting flux qubit. We discuss how to generate the entangled states between the flux qubit and two NVEs by the resonant driving. Then the ECSs of the NVEs can be obtained by projecting the flux qubit, and the entanglement detection can be realized by transferring the quantum state from the NVEs to the flux qubit. Our numerical simulation shows that even under current experimental parameters the concurrence of the ECSs can approach unity. We emphasize that this method is straightforwardly extendable to the case of many NVEs.

As one of the promising building blocks for solid-state quantum information processing (QIP)[1–6], the nitrogen-vacancy (NV) center consisting of a substitutional nitrogen atom and an adjacent vacancy in diamond can be optically controlled and fast microwave manipulated with long coherence time even at room temperature[7,8]. Additionally, benefiting from the enhancement of the magnetic-dipole coupling by a factor $\sqrt{N}$ through the collective excitation, the strong coupling regime has been reached in the hybrid systems consisting of NV center ensemble (NVE) and superconducting circuit[9–17], which have recently attracted much attention. Several potential applications based on the collective excitation of the NVEs are investigated both theoretically and experimentally, such as quantum memories[18–21], continuous variable entanglement[22,23], quantum state transfer[24] and quantum simulation[25].

The practical quantum information processing requires generation of multipartite entanglement among NVEs, which is usually quite complicated and time-consuming. For example, to generate entanglement between two NVEs, we may employ a sequence of single- and two-qubit operations, such as SWAP gates. In this way, either the gate number or the operation time increases much more quickly as the number of the NVEs increases. Therefore, to efficiently generate multipartite entanglement among NVEs, we need to find a faster method with less operation time and gates. To this end, we present in this article a scalable and tunable framework for generating macroscopic arbitrary entangled coherent state (ECS)[26–32] among many separate NVEs in a deterministic way. The key point of our proposal is that the flux qubit plays the role of data bus and the collective excitations of the NVEs behave as bosonic modes or harmonic oscillators in the low-excitation limit. Through the collective magnetic coupling and the *in situ* tunability of the flux qubit, we show that a macroscopic ECS of NVEs can be generated with high success possibilities even under the decoherence of the flux qubit and NVEs. More importantly, we consider the magnetic field applied along a direction [100] of the NV centers[18] to suppress the broadening of the ODMR spectral lines due to excitations in four crystalline orientations. This can largely reduce the overheads in gate operations with the increment of the number of NVEs. So our scheme not only allows an efficient way to accessing the large-scale continuous variable quantum computing in many-body systems, but also serves as a critical building block towards scalable architectures based on solid-state QIP. It should be noted that the ECS owns unique quantum characteristics[33–35] (e.g., robustness to single-particle decoherence) and can be used for various applications beside quantum information processing[36], ranging from the fundamental quantum information theory[37] and the implementation of quantum communication[38,39] to quantum metrology[40]. The quantum error correction may also be easily implemented with the logical qubit defined by the superposition of the coherent states[41,42].

The remainder of this paper is organized as follows. We present our system architecture in details in Sec. II, and the preparation and readout of the ECS of NVEs in Sec. III. Sec. IV focuses on the influence from the decoherence effects of the system. Discussion is presented in Sec. V. Finally, we conclude our findings in Sec. VI.

Results

System and Model. As schematically shown in Fig. 1, we consider two diamond NVEs glued near the boundary of a big superconducting gap-tunable flux qubit, which consists of four Josephson junctions characterized by Josephson energies E_J and αE_J, respectively. Near each of the NVEs, there are small flux qubits employed for detection, which are initially tuned to be uncoupled with both the NVEs and the big flux qubit. When the biasing of the main loop is close to one-half of a flux quantum $\Phi_0 = h/2e$, the gap-tunable flux qubit can be treated as an effective two-level system described by the Hamiltonian (in units of $\hbar = 1$ throughout the paper) $H_f = -\frac{1}{2}[\varepsilon(\Phi_{ext})\sigma_z + \Delta(\Phi'_{ext})\sigma_x]$[18,43], where σ_z and σ_x are usual Pauli operators in the basis of flux eigenstates $|0\rangle_f$(*clockwise* persistent current) and $|1\rangle_f$ (*counterclockwise* persistent current). Here, the energy splitting of the qubit is given by $\hbar\varepsilon(\Phi_{ext}) = 2I_p(\Phi_{ext} - \Phi_0/2)$ with I_p the persistent current in the flux qubit. $\hbar\Delta(\Phi'_{ext})$ is the energy of the tunnel splitting, which induces flip of the qubit states[44,45]. Note that $\varepsilon(\Phi_{ext})$ and $\Delta(\Phi'_{ext})$ can be controlled independently by the external magnetic flux threading the main loop and α loop, respectively, through two extra microwave lines for a finite time period, e.g., of the order of *nanosecond*[46–48]. This enables us to couple the flux qubit to the NVE at the optimal point where the flux qubit has its longest coherence time. In our case we tune $\varepsilon(\Phi_{ext})$ to be zero, and tune $\Delta(\Phi'_{ext})$ to be equal to NVEs' transition frequency. In this way, the flux qubit basis $\{|0\rangle_f, |1\rangle_f\}$ is defined in the eigenstates of the Pauli operator σ_x. Additionally, a resonantly driven microwave on the flux qubit with Rabi frequency Ω_d is also required to control the dynamics of the system.

For the spin-triplet ground state of a NV center with a zero-field splitting $D_{gs} = 2.87$ GHz between $m_S = 0$ and the nearly degenerate sublevels $|m_S = \pm 1\rangle$[49], we apply an external magnetic field $\vec{B}_{ext}$ along the crystalline direction [100] of the NV centers to split the degenerate sublevels $|m_S = \pm 1\rangle$, which results in a two-level system denoted by $|g\rangle = |^3A, m_s = 0\rangle$ and $|e\rangle = |^3A, m_s = -1\rangle$, respectively[16]. So the Hamiltonian of the NVEs is given by

$$H_{NV\,E} = \sum_{j=1}^{2}\sum_{i=1}^{N_j}\left\{D_{gs}\left(S_{z,i}^{j}\right)^2 + E\left[\left(S_{x,i}^{j}\right)^2 - \left(S_{y,i}^{j}\right)^2\right] + g_e\mu_B B_z S_{z,i}^{j}\right\}, \quad (1)$$

where the last term represents the Zeeman splitting under the magnetic field B_z (i.e., the part of the external magnetic field along the crystalline directions). E is the strain-induced splitting, g_e is the ground-state Lander factor, μ_B is the Bohr magneton, and N_j is the number of the NV centers involved in the j-th spin ensemble. To have a good two-level approximation for the NV centers, the diamond crystal is assumed to be bonded on top of the flux qubit chip with its [001] surface facing the chip[18]. $S_{x,i}^{j}$, $S_{y,i}^{j}$, and $S_{z,i}^{j}$ are spin-1 Pauli operators for the i-th NV center in the j-th NVE. Furthermore, we consider the case where the strain-induced fine-structure splitting is negligible compared to the Zeeman splitting, i.e., $\left|E\left[\left(S_{x,i}^{j}\right)^2 - \left(S_{y,i}^{j}\right)^2\right]\right| \ll \left|g_e\mu_B B_z S_{z,i}^{j}\right|$[9,10], and thereby the second term in $H_{NV\,E}$ can be neglected. Considering the subspace spanned by the states $|m_S = 0\rangle$ and $|m_S = -1\rangle$, we have the total Hamiltonian for the whole system as[17]

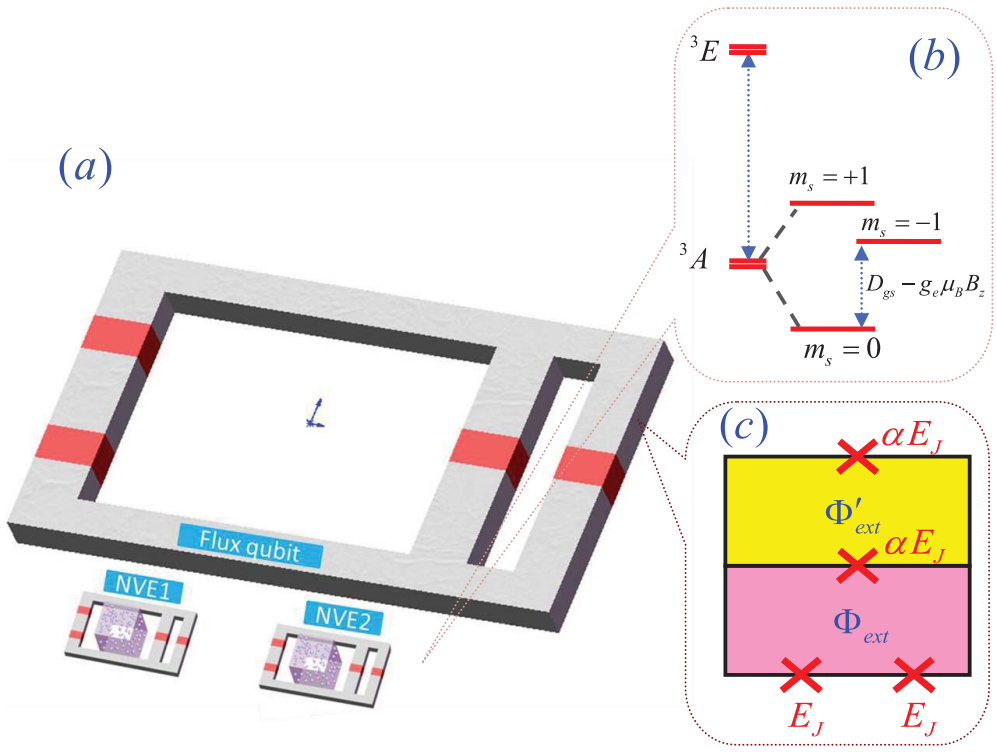

Figure 1 | (a) Schematic of the hybrid system, where two NVEs are attached on the surface of a big flux qubit, and the two small flux qubits nearby are used for entanglement detection. (b) Level structure of a single NV center, where we encode logical states $|g\rangle$ and $|e\rangle$ in $|^3A, m_s = 0\rangle$, and $|^3A, m_s = -1\rangle$, respectively. (c) Schematic of the flux qubit, where the qubit consists of the main loop (inferior pink panel) and four Josephson junctions (red crosses) characterized by Josephson energies E_J and αE_J with $\alpha \approx 0.9$. The magnetic flux through the main loop and the α loop are denoted by Φ_{ext} and Φ'_{ext}, respectively.

$$H_1 = -\frac{1}{2}\Delta(\Phi'_{ext})\sigma_x + \Omega_d \cos(\omega_f t)\sigma_z + \sum_{j=1}^{2}\sum_{i=1}^{N_j}\left[\frac{1}{2}\omega_j \tau_{z,i}^{j} + \frac{1}{\sqrt{2}} g_e \mu_B B^f \tau_{x,i}^{j}\sigma_z\right], \quad (2)$$

where $\omega_j = D_{gs} - g_e\mu_B B_z$, the last term is the interaction between the NVE and the flux qubit, and B^f is the magnetic field (along the direction [001] of the NV centers) produced by the flux qubit. $\tau_{x,i}^{j}$, $\tau_{y,i}^{j}$ and $\tau_{z,i}^{j}$ are the spin-$\frac{1}{2}$ Pauli operators for the i-th NV center in the j-th spin ensemble. Actually, the additional magnetic field B^f is attributed to the superposition state of the *clockwise* and *counter-clockwise* persistent currents. Ω_d (ω_f) is the Rabi frequency (frequency) of the additional microwave resonantly driving on the flux qubit.

Using the Holstein-Primakoff (HP) transformation[50], we map the spin operators to the bosonic operators as follows: $\sum_{i=1}^{N_j}\tau_{+,i}^{j} = \sqrt{N_j}b_j^{+}$, $\sum_{i=1}^{N_j}\tau_{-,i}^{j} = \sqrt{N_j}b_j$ and $\sum_{i=1}^{N_j}\tau_{z,i}^{j} = 2b_j^{+}b_j - N_j$, where the operators b_j and b_j^{+} obey the standard bosonic commutator $\left[b_j, b_j^{+}\right] = 1$ in the weak excitation limit $\left\langle b_j^{\dagger}b_j\right\rangle \ll N_j$. Here we denote the Fock state basis of the bosonic mode b_j as $n|n\rangle_j = b_j^{\dagger}b_j|n\rangle_j$, for j = 1, 2. The coherent state of the mode b_j is defined as $\alpha|\alpha\rangle_j = b_j|\alpha\rangle_j$. Then effective Hamiltonian on the basis of the HP transformations above becomes

$$H_2 = -\frac{\Delta(\Phi'_{ext})}{2}\sigma_x + \Omega_d \cos(\omega_f t)\sigma_z + \sum_{j=1}^{2}\left[\omega_j b_j^{+}b_j + G_j\left(b_j^{+} + b_j\right)\sigma_z\right], \quad (3)$$

where $G_j = \sqrt{N_j/2}\, g_e\mu_B B^f$ is the effective coupling strength between the NVE and the flux qubit. In the case of $G_j \ll \omega_j$ and $\Omega_d \ll \omega_f$, the Hamiltonian in the basis of the eigenstates of the flux qubit takes the form $H_3 = \frac{\Delta(\Phi'_{ext})}{2}\sigma_z + \frac{1}{2}\Omega_d\left(e^{-i\omega_f t}\sigma_+ + e^{i\omega_f t}\sigma_-\right) + \sum_{j=1}^{2}\left[\omega_j b_j^{+}b_j + G_j\left(b_j^{+}\sigma_- + b_j\sigma_+\right)\right]$, where the rotating-wave approximation (RWA) is adopted to neglect fast oscillating terms. The ladder operators $\sigma_\pm$ are defined as $\sigma_\pm = (\sigma_z \pm i\sigma_y)/2$.

Preparation and readout of the ECS. In what follows, we describe how to generate deterministically the ECS of two spin ensembles in our setup by following three steps:

(*i*) The system is initially prepared in the state $|\psi(0)\rangle = |0\rangle_f|0\rangle_1|0\rangle_2$. Assuming that the splitting frequency $\Delta(\Phi'_{ext})$ of the flux qubit and the frequency ω_f of the driving field are set to be equal to the NVE collective excitation frequency ω_j, the effective Hamiltonian in the rotating frame becomes $H_4 = \sum_{j=1}^{2} G_j\left(b_j^{+}\sigma_- + b_j\sigma_+\right)$. At this step, $\Omega_d(t)$ in Eq. (3) is set to be zero.

(*ii*) Turning on the drive $\Omega_d(t)$ from zero to Ω_d ($G_j \ll \Omega_d \ll \omega_j$) on the time scale of nanoseconds, we can switch from the flux qubit basis $\{|0\rangle_f, |1\rangle_f\}$ to the dressed state basis $\{|+\rangle_f, |-\rangle_f\}$, with $|\pm\rangle_f = \left(|0\rangle_f \pm |1\rangle\right)_f/\sqrt{2}$, and the evolution operator takes the form $U(t) = U_0 \exp\left\{-it\left[\sum_{j=1}^{2}\frac{G_j}{2}\left(b_j^{+} + b_j\right)\tilde{\sigma}_z\right]\right\}$ after neglecting the fast oscillating terms, with $\tilde{\sigma}_z = |+\rangle\langle +| - |-\rangle\langle -|$, and $U_0 = \exp(-it\Omega_d\tilde{\sigma}_z/2)$ is the rotating unitary operator. This operation $U(t)$ displaces the collective bosonic mode of NVE by the amount of $\pm iG_j t/2$ conditional on the flux qubit states $|0\rangle_f$ or $|1\rangle_f$, and this complex amplitude $iG_j t/2$ is proportional to the evolution time. As a result, the system state $|\psi(0)\rangle$ evolves into $|\psi(t)\rangle = \left[e^{-it\Omega_d/2}|+\rangle_f|\alpha_1\rangle_1|\alpha_2\rangle_2 + e^{it\Omega_d/2}|-\rangle|-\alpha_1\rangle_1|-\alpha_2\rangle_2\right]/\sqrt{2}$ with $\alpha_1 = -iG_1 t/2$ and $\alpha_2 = -iG_2 t/2$. For simplicity we set the phase factor $\Omega_d t/2 = n\pi$ ($n = 1,2,3\cdots$), which can be realized by precisely controlling the operation time. One can see the generated entanglement among the flux qubit and the two NVEs.

(*iii*) To generate the ECS of NVEs, we need to measure the state of the flux qubit on $|0\rangle_f$ and $|1\rangle_f$. This task can be performed by applying a pulse sequence on a *dc* SQUID attached to the flux qubit (not shown in Fig. 1), where the voltage state of the SQUID is very sensitive to the faint change of the flux, and depends on the switching probability of the energy eigenstates of the flux qubit[16]. So the two NVEs will be projected into the ECS $|\psi_-\rangle = |\alpha_1\rangle_1|\alpha_2\rangle_2 - |-\alpha_1\rangle_1|-\alpha_2\rangle_2$ or $|\psi_+\rangle = |\alpha_1\rangle_1|\alpha_2\rangle_2 + |-\alpha_1\rangle_1|-\alpha_2\rangle_2$, corresponding to the readout from the state $|1\rangle_f$ or $|0\rangle_f$ with respect to the flux qubit, respectively. This implies that each ECS is created with the success possibility of 100% if the projection measurement is perfect.

The detection of the ECS is not a trivial task. In order to measure the ECS, we need to transfer the states from the NVEs to two additional small flux qubits, each of which is attached on a NVE, as shown in Fig. 1. So the task of entanglement detection can be performed by the direct measurement on the states of flux qubits. Here the qubit states in NVE are defined as $|\bar{0}\rangle_j = \left(|\alpha_j\rangle_j + |-\alpha_j\rangle_j\right)\Big/\sqrt{2+2\exp\left[-2|\alpha_j|^2\right]}$, and $|\bar{1}\rangle_j = \left(|\alpha_j\rangle_j - |-\alpha_j\rangle_j\right)\Big/\sqrt{2-2\exp\left[-2|\alpha_j|^2\right]}$ with j = 1, 2, respectively[36]. It is easy to verify that $|\bar{0}\rangle_j$ and $|\bar{1}\rangle_j$ are orthogonal to each other once $|\alpha_j| > 0$. In the limit of $|\alpha_j|^2 \ll 1$, the coherent qubit states can be approximated as a superposition of Fock states $|\bar{0}\rangle = \sqrt{2+2\exp\left[-2|\alpha_j|^2\right]}|0\rangle + O\left(\alpha_j^2\right)|2\rangle$ and $|\bar{1}\rangle = \sqrt{2-2\exp\left[-2|\alpha_j|^2\right]}|1\rangle + O\left(|\alpha_j|^2\right)|3\rangle$. Therefore, in the case of $|\alpha_j|^2 \ll 1$, we can transfer the state from NVEs to flux qubits in the Fock state basis using the SWAP gate between the j-th NVE and the j-th flux qubit.

For a more general case of $|\alpha_j|^2 > 1$, the usual way to the state transfer from the j-th NVE to the j-th flux qubit, $\left(\cos\theta|\bar{0}\rangle_j + \sin\theta|\bar{1}\rangle_j\right)\otimes|0\rangle_{fj} \rightarrow |\bar{1}\rangle_j \otimes \left(\cos\theta|0\rangle_{fj} + \sin\theta|1\rangle_{fj}\right)$, can be performed by a sequence of single-qubit gates and the operation[36]

$$U_s = \exp\left[i\varepsilon\left(b_j^{\dagger} + b_j\right)|1\rangle_{fj}\langle 1|\right]\exp\left(i\pi\sigma_z^j/2\right)\exp\left(-i\pi b_j^{\dagger}b_j\sigma_y^j\right), \quad (4)$$

where the operator $\exp\left(-i\pi b_j^{\dagger}b_j\sigma_y^j\right)$ plays the role of flipping the flux qubit, achievable by first applying a single-qubit rotation and then by performing the operation $\exp\left(-i\pi b_j^{\dagger}b_j\sigma_x^j\right)$ on the flux qubit. Alternatively, the operations above can be accomplished by the following method. Suppose that the effective Hamiltonian between the NVEs and the small flux qubit is similar to Eq. (3) but without the microwave drive Ω_d. So the corresponding operation is $\exp\left[-it\chi_j b_j^{\dagger}b_j\sigma_x^j\right]$, where $\chi_j = G_j^2/\Delta_j$, and Δ_j is the detuning between the transition frequencies of the j-th small flux qubit and the j-th NVE. Additionally, the operation $\exp\left[i\varepsilon_i\left(b_j^{\dagger} + b_j\right)|1\rangle_{fj}\langle 1|\right]$ with $\varepsilon_j = \pi/(2\alpha_j)$ is actually the conditional displacement of the bosonic mode if and only if the flux qubit is in the excited state $|1\rangle_{fj}$. Such conditional displacements have been achieved by Eq. (3) with a strong microwave drive. Hence the operation U_s should be achievable with currently experimental technology, and then the

entanglement between NVEs can be detected by measuring the states of small flux qubits.

We should note that the detection in our scheme requires the coupling strength of each NV center to the large flux qubit to be proportional to that to the small one, which guarantees the collective mode detected by the small flux qubit to be identical to that already prepared in the large flux qubit. Although it looks like an additional technical difficulty, the operations are experimentally doable. For example, the NVEs can be placed to the positions where the magnetic fields generated by both the small and the large flux qubits are nearly homogenous due to careful design of the qubits' circuit patterns[51].

Discussion

To visualize the decoherence effect on the evolution of concurrence between the NVEs, we have plotted the time-dependent $C_{12}(t)$ in Fig. 2. Due to the presence of decoherence, the concurrence increases first and then decreases gradually to zero. So to carry out our scheme more efficiently, we have to suppress these imperfect factors as much as we can. On the other hand, the concurrence keeps to be of very high values (≥ 0.95) under the decoherence as long as the time is evaluated within the domain $[2/G, 2.5/G]$, and the maximal entanglement ($\simeq 0.97$) can be obtained if the operation time $t'_{op} \simeq 2.3/G$. We emphasize that a stronger decoherence only slightly reduces the maximal value of the concurrence, as shown in the bottom panel of Fig. 2.

In Fig. 3, we have exactly calculated the evolution of the system, where the fast oscillating terms are involved. We may compare the generated ECS $|\psi'(t)\rangle$ in the non-RWA case with the ECS $|\psi(t)\rangle$ generated by the effective unitary operator $U(t) = U_0 \exp\left\{-it\left[\sum_{j=1}^{2}\frac{G_j}{2}\left(b_j^{+}+b_j\right)\tilde{\sigma}_z\right]\right\}$. Here, the fidelity is defined as $F(t) = |\langle\psi'(t)|\psi(t)\rangle|$. As shown in Fig. 3, the fidelity $F(t)$ decreases in time evolution, which is larger than 0.98 only for $t_0 \leq 2/G$ and $\Omega/G = 30$. Therefore, effective unitary operator $U(t)$ is valid within this regime, and the generated ECS has the amplitude $|\alpha| = |\beta| = |it_0G/2| = 1$ at time t_0, which is large enough to define the orthogonal qubit. In practice, if we choose $G = 25$ MHz, the microwave drive is $\Omega = 750$ MHz, which is within the reach of experimental feasibility[55].

The condition on HP transformation for the NVEs requires that the total number of the excitations be much smaller than the number of the NV centers in each NVE. In our case, the average photon number in the two NVEs can be calculated as

$$N_1 = |\alpha|^2\xi/S, \qquad N_2 = |\beta|^2\xi/S, \tag{5}$$

where $\xi = e^{-\gamma t} + e^{\gamma t} - 2qP_1P_2\cos(\Omega_d t)$. Considering the case of $G_1 \neq G_2$, we set $G_2 = (1+\Delta)G_1$. As shown in Fig. 4, we plot the total photon number $N = N_1 + N_2$ as a function of the parameter Δ and time. One can find that the value of N is smaller than 20. So the small excitation number ensures a reasonable HP transformation in our scheme.

We address some remarks for experimental implementation of our scheme. In our proposal, the flux qubit is strongly driven and

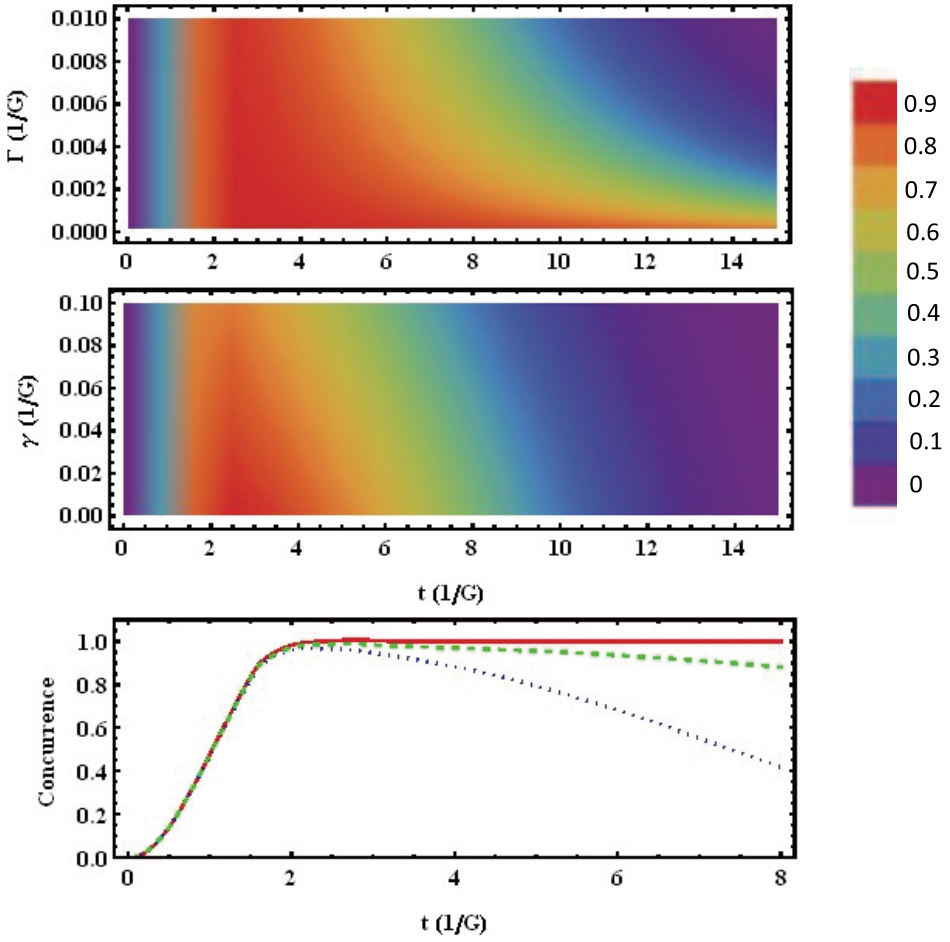

Figure 2 | Top: Density plot of the concurrence of the ECS versus the dimensionless parameters Γ and t, where $\gamma = 0.01$. Middle: Density plot of the concurrence of the ECS versus the dimensionless parameters γ and t, where $\Gamma = 0.01$. Bottom: Concurrence of the ECS versus the dimensionless time t, where the solid, dashed, and dotted lines denote $\Gamma = \gamma = 0$, $\Gamma = \gamma/10 = 0.001$, and $\Gamma = \gamma = 0.01$, respectively. Here we have used the method in[54] to calculate the concurrence in the case of $\Gamma = \gamma = 0$. $\Omega_d = 15$ and $G_1 = G_2 = 1$ are assumed in all panels.

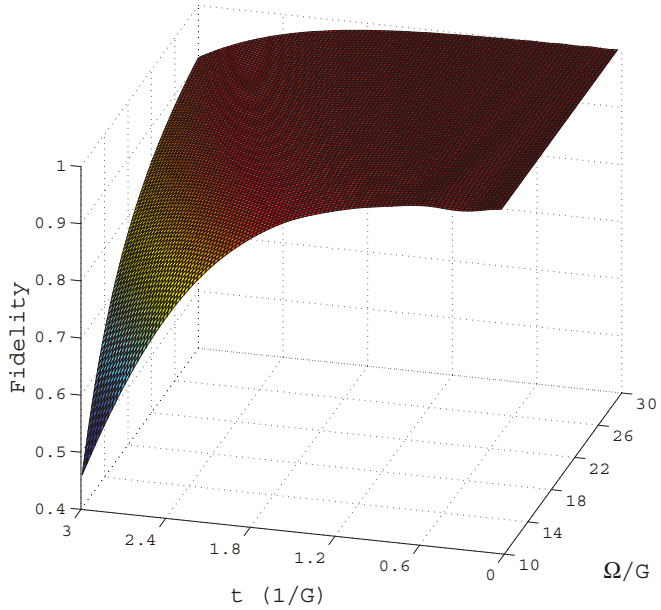

Figure 3 | Time evolution of the fidelity $F(t) = |\langle\psi'(t)|\psi(t)\rangle|$ of the generated ECS versus the time and the parameter Ω. Here we suppose $G_1 = G_2$ for simplicity.

the qubit basis is changed to dressed states $|+\rangle$ and $|-\rangle$. This is equivalent to the continuous dynamical decoupling[21]. Based on recent experiments[16], the NVE-flux qubit coupling strength has reached up to 70 MHz. In our proposal, if we set $G_1 = G_2 =$ 50 MHz and $t'_{op} = 2.3/G$, the operation time for obtaining the ECS of NVEs with high values of concurrence is about 40 ns, which is much shorter than the coherence times of the NV centers and the flux qubit. In addition, the decoherence of the NVE increases with the density of the NV centers. Thus, it is required to suppress the decoherence of the NVE by the spin-echo pulses and/or by improving the conversion rate from nitrogen to NV which decrease the redundant nitrogen spins and thereby reduce the linewidth of the NVEs.

As a final remark, we emphasize that the setup plotted in Fig. 1 is straightforwardly extendable to the case with many NVEs involved, which would be essential to scalable QIP. For a more specific description, we have designed in Fig. 5 a novel tunable architecture that allows superconducting flux qubits to provide flexibility in arrangement of NVEs. In such a way, all spin ensembles are arranged in two or three spatial dimensions, where the flux qubit serves as a quantum bus for the non-interacting spin ensembles. The total Hamiltonian is given by

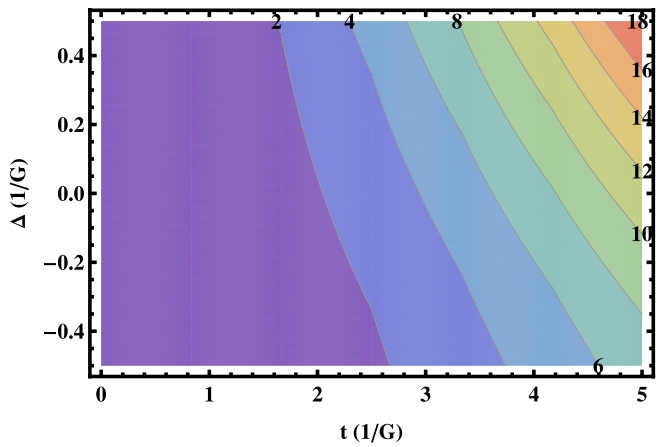

Figure 4 | The total photon number N in two NVEs as a function of the parameter Δ and the dimensionless time, where we set $\gamma = \Gamma = 0.01$, $\kappa = 0.04$, $G_1 = 1$, and $\Omega_d = 5$.

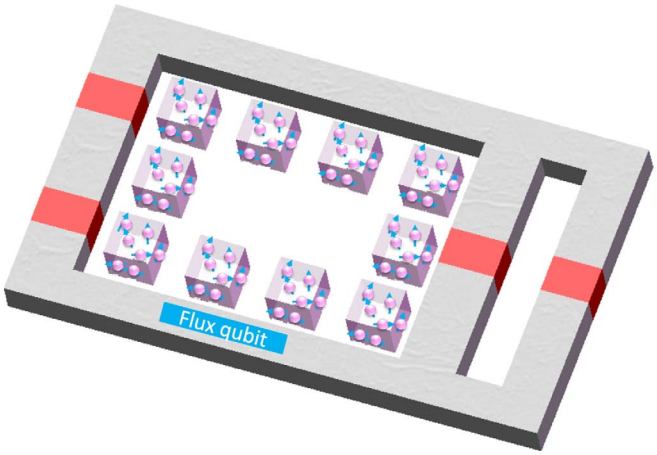

Figure 5 | Schematic of the preparation of ECS with many NVEs, where all the NVEs are attached on the surface of a flux qubit.

$$H_N = -\frac{\Delta(\Phi'_{ext})}{2}\sigma_x + \Omega_d \cos(\omega_f t)\sigma_z + \sum_{j=1}^{N}\left[\omega_j b_j^+ b_j + G_j\left(b_j^+ + b_j\right)\sigma_z\right], \quad (6)$$

with N the total number of NVEs. Eq. (6) can take an effective form $\sum_{j=1}^{N}\frac{G_j}{2}\left(b_j^+ + b_j\right)\tilde{\sigma}_z + \frac{1}{2}\Omega_d\tilde{\sigma}_z$ in the dressed state basis by performing the similar transformations to the two-NVE case. As a result, all the NVEs will be projected into the ECS

$$|\psi_{\pm}^N\rangle = \frac{1}{Y}\left(|\alpha_1\rangle_1|\alpha_2\rangle_2\cdots|\alpha_N\rangle_N \pm |-\alpha_1\rangle_1|-\alpha_2\rangle_2\cdots|-\alpha_N\rangle_N\right) \quad (7)$$

with the normalization factor Y, and $\alpha_j = -iG_jt/2$ corresponding to the readout from the states $|0\rangle_f$ and $|1\rangle_f$ with respect to the flux qubit, respectively. We note that optical pulses are required to individually address the NVEs in the spatial scale. The present method would be very efficient for generating a continuous-variable entanglement among separate spin ensembles, which is a necessary step on the path towards a scalable solid-state quantum computing.

In summary, we have proposed a scheme of one-step creation of arbitrary macroscopic ECSs among many separate NVEs through the collective magnetic coupling to the flux qubit. We have shown that the ECSs of the spin ensembles can be achieved with high success possibilities even under the influence of decoherence from the flux qubit and NVEs. We have realized the worry about the large loop of the flux qubit which may cause more noise. However, we consider that the gap-tunable flux qubit employed in our scheme can work at the optimal point, strongly suppressing the dephasing time. On the other hand, we have recently fabricated some large loop gap-tunable flux qubits experimentally with the coherent time on the order of one microsecond, in which no significant drop was observed when the flux qubit loop size is increased from 4×5 μm^2 to 20×20 μm^2. Considering the fact that we can use small pieces of NV sample with the size about 1×1 μm^2, we are confident of the feasibility of a multi-qubit entanglement using a flux qubit with the loop size of 400 μm^2. Therefore we argue that the proposal is practical under the present experimental parameters, and should be helpful for large-scale QIP in solid-state quantum systems, particularly for continuous-variable quantum computing and quantum communication.

Method

Modeling of decoherence effects. From now on we analyze the influence from decoherence of the flux qubit and the NVEs. Below we may focus on the decoherence effect in the step (*ii*) using the master equation

$$\begin{aligned}\dot{\rho}(t) &= -i\left[\sum_{j=1}^{2}\frac{G_j}{2}\left(b_j^+ + b_j\right)\tilde{\sigma}_z + \frac{1}{2}\Omega_d\tilde{\sigma}_z, \rho(t)\right] + \mathcal{L}\rho(t),\\ \mathcal{L}\rho(t) &= \sum_{j=1}^{2}\frac{\Gamma}{2}\left(2b_j\rho(t)b_j^+ - b_j^+ b_j\rho(t) - \rho(t)b_j^+ b_j\right)\\ &\quad + \frac{\gamma}{2}(2\tilde{\sigma}_-\rho(t)\tilde{\sigma}_+ - \tilde{\sigma}_+\tilde{\sigma}_-\rho(t) - \rho(t)\tilde{\sigma}_+\tilde{\sigma}_-),\end{aligned} \tag{8}$$

where γ (Γ) is the decay rate of the flux qubit (NVE). For simplicity, we have assumed $\Gamma_1 = \Gamma_2 = \Gamma$. Using the superoperator technique[52] and Hausdorff similarity transformation[53], we deduce the following differential equations with respect to the density matrix of the flux qubit,

$$\begin{aligned}\dot{\rho}_{++}(t) &= -i\left[\frac{G_j}{2}\left(b_1 + b_1^+\right) + \frac{G_j}{2}\left(b_2 + b_2^+\right) + \frac{1}{2}\Omega_d\rho_{++}(t)\right]\\ &\quad + \mathcal{L}'\rho_{++}(t) - \gamma\rho_{++}(t),\\ \dot{\rho}_{+-}(t) &= -i\left\{\frac{G_j}{2}\left(b_1 + b_1^+\right) + \frac{G_j}{2}\left(b_2 + b_2^+\right) + \frac{1}{2}\Omega_d\rho_{+-}(t)\right\}\\ &\quad + \mathcal{L}'\rho_{+-}(t) - \frac{\gamma}{2}\rho_{+-}(t),\\ \dot{\rho}_{-+}(t) &= i\left\{\frac{G_j}{2}\left(b_1 + b_1^+\right) + \frac{G_j}{2}\left(b_2 + b_2^+\right) + \frac{1}{2}\Omega_d\rho_{-+}(t)\right\}\\ &\quad + \mathcal{L}'\rho_{-+}(t) - \frac{\gamma}{2}\rho_{-+}(t),\\ \dot{\rho}_{--}(t) &= i\left[\frac{G_j}{2}\left(b_1 + b_1^+\right) + \frac{G_j}{2}\left(b_2 + b_2^+\right) + \frac{1}{2}\Omega_d\rho_{--}(t)\right]\\ &\quad + \mathcal{L}'\rho_{--}(t) + \gamma\rho_{++}(t),\\ \mathcal{L}'\rho(t) &= \sum_{j=1}^{2}\frac{\Gamma}{2}\left(2b_j\rho(t)b_j^+ - b_j^+ b_j\rho(t) - \rho(t)b_j^+ b_j\right).\end{aligned} \tag{9}$$

Then we solve the differential equations above with the initial state $|\psi(t_1)\rangle = \left(|+\rangle_f + |-\rangle_f\right)|0\rangle_1|0\rangle_2/\sqrt{2}$ and obtain

$$\begin{aligned}\rho(t) &= \left(e^{-\gamma t}|+,\alpha,\beta\rangle\langle+,\alpha,\beta| + qe^{-i\Omega_d t}|+,\alpha,\beta\rangle\langle-\alpha,-\beta|\right.\\ &\quad + qe^{i\Omega_d t}|-,-\alpha,-\beta\rangle\langle+,\alpha,\beta|\\ &\quad \left. + e^{\gamma t}|-,-\alpha,-\beta\rangle\langle-,-\alpha,-\beta|\right)/2,\end{aligned} \tag{10}$$

where $q = \exp\left[-\frac{\gamma t}{2} - \left(G_1^2 + G_2^2\right)\left(\Gamma t + 4e^{-\Gamma t/2} - e^{-\Gamma t} - 3\right)/\Gamma^2\right]$ is a factor reflecting the competition between the spin-boson coupling and the dissipation.

After the step (iii), the final state of the NVEs, with the readout of the flux qubit being $|0\rangle_f$, turns to be

$$\begin{aligned}\rho_{NV\,Es} &= \frac{1}{S}\left[e^{-\gamma t}|\alpha,\beta\rangle\langle\alpha,\beta| + qe^{-i\Omega_d t}|\alpha,\beta\rangle\langle-\alpha,-\beta|\right.\\ &\quad + qe^{i\Omega_d t}|-\alpha,-\beta\rangle\langle\alpha,\beta|\\ &\quad \left. + e^{\gamma t}|-\alpha,-\beta\rangle\langle-\alpha,-\beta|\right],\end{aligned} \tag{11}$$

where $S = e^{-\gamma t} + e^{\gamma t} + 2qP_1P_2\cos(\Omega_d t)$ is the normalization constant with $P_1 = \langle\alpha|-\alpha\rangle$ and $P_2 = \langle\beta|-\beta\rangle$. Note that we can obtain the similar result if the readout of the flux qubit is $|1\rangle_f$.

We employ below the concept of concurrence for bipartite entangled nonorthogonal states[54] to measure entanglement between the NVEs. To this end, we first make a suitable transformation on Eq. (11) from the nonorthogonal form of Eq. (11) into an orthogonal form by rebuilding two orthogonal and normalized states as the basis states of the two-dimensional Hilbert space, i.e., we define $|0\rangle_1 = |\alpha\rangle_1$, $|1\rangle_1 = (|-\alpha\rangle_1 - P_1|\alpha\rangle_1)/M_1$ with $M_1 = \sqrt{1-|P_1|^2}$ for NVE1, and $|0\rangle_2 = |\beta\rangle_2$, $|1\rangle_2 = (|-\beta\rangle_2 - P_2|\beta\rangle_2)/M_2$ with $M_2 = \sqrt{1-|P_2|^2}$ for NVE2. Then the reduced density operator (Eq. (11)) in the new basis states is rewritten as

$$\rho'_{NV\,Es} = \frac{1}{S}\begin{pmatrix} e^{-\gamma t} + 2qP_1P_2\cos(\Omega_d t) & P_1M_2(e^{\gamma t}P_1P_2 & P_2M_1(e^{\gamma t}P_1P_2 & M_1M_2(e^{\gamma t}P_1P_2\\ & + e^{\gamma t}P_1^2P_2^2 & + qe^{-i\Omega_d t}) & + qe^{-i\Omega_d t}) & + qe^{-i\Omega_d t})\\ P_1M_2\left(e^{\gamma t}P_1P_2 + qe^{i\Omega_d t}\right) & e^{\gamma t}P_1^2M_2^2 & e^{\gamma t}P_1P_2M_1M_2 & e^{\gamma t}P_1M_1M_2^2\\ P_2M_1\left(e^{\gamma t}P_1P_2 + qe^{i\Omega_d t}\right) & e^{\gamma t}P_1P_2M_1M_2 & e^{\gamma t}P_2^2M_1^2 & e^{\gamma t}P_2M_1^2M_2\\ M_1M_2\left(e^{\gamma t}P_1P_2 + qe^{i\Omega_d t}\right) & e^{\gamma t}P_1M_1M_2^2 & e^{\gamma t}P_2M_1^2M_2 & e^{\gamma t}M_1^2M_2^2 \end{pmatrix} \tag{12}$$

So we have the concurrence for the ECS in the form

$$C_{12}(t) = \max\{0, 2M_1M_2q/S\}. \tag{13}$$

1. Childress, L. *et al.* Coherent dynamics of coupled electron and nuclear spin qubits in diamond. *Science* **314**, 281 (2006).
2. Dutt, M. V. G. *et al.* Quantum register based on individual electronic and nuclear spin qubits in diamond. *Science* **316**, 1312 (2007).
3. Jiang, L. *et al.* Repetitive readout of a single electronic spin via quantum logic with nuclear spin ancillae. *Science* **326**, 267 (2009).
4. Neumann, P. *et al.* Single-shot readout of a single nuclear spin. *Science* **329**, 542 (2010).
5. Neumman, P. *et al.* Quantum register based on coupled electron spins in a room-temperature solid. *Nature Phys.* **6**, 249 (2010).
6. Togan, E. *et al.* Quantum entanglement between an optical photon and a solid-state spin qubit. *Nature* **466**, 730 (2010).
7. Balasubramanian, G. Ultralong spin coherence time in isotopically engineered diamond. *Nat. Materials* **8**, 383 (2009).
8. Mizuochi, N. Coherence of single spins coupled to a nuclear spin bath of varying density. *Phys. Rev. B* **80**, 041201 (2009).
9. Xiang, Z. L., Ashhab, S., You, J. Q. & Nori, F. Hybrid quantum circuits: Superconducting circuits interacting with other quantum systems. *Rev. Mod. Phys.* **85**, 623 (2013).
10. Xiang, Z. L., Lü, X. Y., Li, T. F., You, J. Q. & Nori, F. Hybrid quantum circuit consisting of a superconducting flux qubit coupled to a spin ensemble and a transmission-line resonator. *Phys. Rev. B* **87**, 144516 (2013).
11. Kubo, Y. *et al.* Strong coupling of a spin ensemble to a superconducting resonator. *Phys. Rev. Lett.* **105**, 140502 (2010).
12. Schuster, D. I. *et al.* High-cooperativity coupling of electron-spin ensembles to superconducting cavities. *Phys. Rev. Lett.* **105**, 140501 (2010).
13. Amsüss, R. *et al.* Cavity QED with magnetically coupled collective spin states. *Phys. Rev. Lett.* **107**, 060502 (2011).
14. Kubo, Y. *et al.* Hybrid quantum circuit with a superconducting qubit coupled to a spin ensemble. *Phys. Rev. Lett.* **107**, 220501 (2011).
15. Kubo, Y. *et al.* Storage and retrieval of a microwave field in a spin ensemble. *Phys. Rev. A* **85**, 012333 (2012).
16. Zhu, X. *et al.* Coherent coupling of a superconducting flux qubit to an electron spin ensemble in diamond. *Nature* **478**, 221 (2011).
17. Marcos, D. *et al.* Coupling nitrogen-vacancy centers in diamond to superconducting flux qubits. *Phys. Rev. Lett.* **105**, 210501 (2010).
18. Saito, S. *et al.* Towards realizing a quantum memory for a superconducting qubit: Storage and retrieval of quantum states. *Phys. Rev. Lett.* **111**, 107008 (2013).
19. Julsgaard, B., Grezes, C., Bertet, P. & Mølmer, K. Quantum memory for microwave photons in an inhomogeneously broadened spin ensemble. *Phys. Rev. Lett.* **110**, 250503 (2013).
20. Yang, W. L., Yin, Z. Q., Hu, Y., Feng, M. & Du, J. F. High-fidelity quantum memory using nitrogen-vacancy center ensemble for hybrid quantum computation. *Phys. Rev. A* **84**, 010301(R) (2011).
21. Cai, J., Jelezko, F., Katz, N., Retzker, A. & Plenio, M. B. Long-lived driven solid-state quantum memory. *New. J. Phys.* **14**, 093030 (2012).
22. Yang, W. L., Yin, Z. Q., Chen, Q., Chen, C. Y. & Feng, M. Two-mode squeezing of distant nitrogen-vacancy-center ensembles by manipulating the reservoir. *Phys. Rev. A* **85**, 022324 (2012).
23. Ma, S. L., Li, P. B., Fang, A. P., Gao, S. Y. & Li, F. L. Dissipation-assisted generation of steady-state single-mode squeezing of collective excitations in a solid-state spin ensemble. *Phys. Rev. A* **88**, 013837 (2013).
24. Chen, Q., Yang, W. L. & Feng, M. Controllable quantum state transfer and entanglement generation between distant nitrogen-vacancy-center ensembles coupled to superconducting flux qubits. *Phys. Rev. A* **86**, 022327 (2012).
25. Yang, W. L. *et al.* Quantum simulation of an artificial Abelian gauge field using nitrogen-vacancy-center ensembles coupled to superconducting resonators. *Phys. Rev. A* **86**, 012307 (2012).
26. Sanders, B. C. Entangled coherent states. *Phys. Rev. A* **45**, 6811 (1992).
27. Zhang, W. M., Feng, D. H. & Gilmore, R. Coherent states: Theory and some applications. *Rev. Mod. Phys.* **62**, 867 (1990).
28. Chen, M. Y., Tu, M. W. Y. & Zhang, W. M. Entangling two superconducting LC coherent modes via a superconducting flux qubit. *Phys. Rev. B* **80**, 214538 (2009).
29. Chen, Q., Yang, W. L. & Feng, M. Generation of macroscopic entangled coherent states for distant ensembles of polar molecules via effective coupling to a superconducting charge qubit. *Phys. Rev. A* **86**, 045801 (2012).
30. Zhou, L. & Xiong, H. A macroscopical entangled coherent state generator in a V configuration atom system. *J. Phys. B: At. Mol. Opt. Phys.* **41**, 025501 (2008).
31. Jia, L. J., Yang, Z. B., Wu, H. Z. & Zheng, S. B. Generation of cluster states for cavity fields. *Chin. Phys. B* **17**, 4207 (2008).
32. Munro, W. J., Milburn, G. J. & Sanders, B. C. Entangled coherent-state qubits in an ion trap. *Phys. Rev. A* **62**, 052108 (2000).
33. Lukin, M. D., Yelin, S. F. & Fleischhauer, M. Entanglement of atomic ensembles by trapping correlated photon states. *Phys. Rev. Lett.* **84**, 4232 (2000).

34. Braunstein, S. L. & Kimble, H. J. Teleportation of continuous quantum variables. *Phys. Rev. Lett.* **80**, 869 (1998).
35. Nielsen, M. A. & Chuang, I. L. *Quantum computing and Quantum Information* (Cambridge University Press, Cambridge, UK, 2000).
36. Munro, W. J., Milburn, G. J. & Sanders, B. C. Entangled coherent-state qubits in an ion trap. *Phys. Rev. A* **62**, 052108 (2000).
37. Jeong, H., Paternostro, M. & Ralph, T. C. Failure of local realism revealed by extremely-coarse-grained measurements. *Phys. Rev. Lett.* **102**, 060403 (2009).
38. Park, K. & Jeong, H. Entangled coherent states versus entangled photon pairs for practical quantum-information processing. *Phys. Rev. A* **82**, 062325 (2010).
39. Azuma, K. & Kato, G. Optimal entanglement manipulation via coherent-state transmission. *Phys. Rev. A* **85**, 060303(R) (2012).
40. Joo, J., Munro, W. J. & Spiller, T. P. Quantum metrology with entangled coherent states. *Phys. Rev. Lett.* **107**, 083601 (2011).
41. Leghtas, Z., Kirchmair, G., Vlastakis, B., Schoelkopf, R. J., Devoret, M. H. & Mirrahimi, M. Hardware-efficient autonomous quantum memory protection. *Phys. Rev. Lett.* **111**, 120501 (2013).
42. Vlastakis, B. *et al.* Deterministically encoding quantum information using 100-photon Schrödinger cat states. *Science* **342**, 607 (2013).
43. Stern, M. *et al.* Flux qubits with long coherence times for hybrid quantum circuits. *Phys. Rev. Lett.* **113**, 123601 (2014).
44. Chiorescu, I., Bertet, P., Semba, K., Nakamura, Y., Harmans, C. J. P. M. & Mooij, J. E. Coherent dynamics of a flux qubit coupled to a harmonic oscillator. *Nature* **431**, 159 (2004).
45. Qiu, Y., Xiong, W., Tian, L. & You, J. Q. Coupling spin ensembles via superconducting flux qubits. *Phys. Rev. A* **89**, 042321 (2014).
46. Zhu, X. B., Kemp, A., Saito, S. & Semba, K. Coherent operation of a gap-tunable flux qubit. *Appl. Phys. Lett.* **97**, 102503 (2010).
47. Paauw, F. G., Fedorov, A., Harmans, C. J. P. M. & Mooij, J. E. Tuning the gap of a superconducting flux qubit. *Phys. Rev. Lett.* **102**, 090501 (2009).
48. Fedorov, A., Feofanov, A. K., Macha, P., Díaz, P. F., Harmans, C. J. P. M. & Mooij, J. E. Strong coupling of a quantum oscillator to a flux qubit at its symmetry point. *Phys. Rev. Lett.* **105**, 060503 (2010).
49. Manson, N. B., Harrison, J. P. & Sellars, M. J. Nitrogen-vacancy center in diamond: Model of the electronic structure and associated dynamics. *Phys. Rev. B* **74**, 104303 (2006).
50. Hammerer, K., Sørensen, A. S. & Polzik, E. S. Quantum interface between light and atomic ensembles. *Rev. Mod. Phys.* **82**, 1041 (2010).
51. Zhu, X. B. in *preparation*.
52. Faria, J. G. P. D. & Nemes, M. C. Dissipative dynamics of the Jaynes-Cummings model in the dispersive approximation: Analytical results. *Phys. Rev. A* **59**, 3918 (1999).
53. Witschel, W. Ordered products of exponential operators by similarity transformations. *Int. J. Quantum Chem.* **20**, 1233 (1981).
54. Wang, X. G. Bipartite entangled non-orthogonal states. *J. Phys. A* **35**, 165 (2002).
55. Yoshihara, F., Nakamura, Y., Yan, F., Gustavsson, S., Bylander, J., Oliver, W. D. & Tsai, J. S. Flux qubit noise spectroscopy using Rabi oscillations under strong driving conditions. *Phys. Rev. B* **89**, 020503(R) (2014).

Acknowledgments

The authors thank Jun-Hong An and Naheed Akhtar for enlightening discussions and for their serious reading of the manuscript before submission. This work is supported partially by the National Fundamental Research Program of China under Grant No. 2012CB922102 and No. 2013CB921803, by the NNSF of China under Grants No. 11274351, No. 11274352, No. 11104326. ZQY was supported by the NBRPC (973 Program) 2011CBA00300 (2011CBA00302), NNSFC 11105136, 61361136003, and 61033001.

Author contributions

W.L.Y., Z.Q.Y. and X.B.Z. conceive the idea. W.L.S., Z.Q.Y. and W.L.Y. carry out the research with input from X.B.Z. and F.Z. W.L.S., Z.Q.Y., W.L.Y., X.B.Z., F.Z. and M.F. discuss the results. W.L.S., W.L.Y. and Z.Q.Y. write the manuscript with comments and refinements from X.B.Z. and M.F.

Additional information

Competing financial interests: The authors declare no competing financial interests.

How to cite this article: Song, W.-L. *et al.* One-step generation of multipartite entanglement among nitrogen-vacancy center ensembles. *Sci. Rep.* **5**, 7755; DOI:10.1038/srep07755 (2015).